BioMetals **15:** 325–339, 2002.

Review

Chemical aspects of siderophore mediated iron transport

Hakim Boukhalfa & Alvin L. Crumbliss*
*Department of Chemistry, Duke University, Durham, NC 27708-0346, USA; *Author for correspondence (Tel.: 919-660-1540; Fax: 919-660-1605; E-mail: alc@chem.duke.edu)*

Received 16 January 2002; Accepted 24 January 2002

Key words: bioavailability, coordination chemistry, iron, kinetics, ligand exchange, mechanism, metals, oxidation-reduction, recognition, siderophore, thermodynamics, transport

Abstract

In this mini-review we describe selected aspects of the coordination chemistry relevant to siderophore mediated iron transport and bioavailability. Specific emphasis is placed on a discussion of *in vitro* kinetic and thermodynamic data that are relevant to elucidating possible *in vivo* mechanisms for environmental iron acquisition by microbial cells.

Introduction

Microbial iron bioavailability is largely controlled by the presence of chelating agents that are able to solubilize environmental iron hydroxides and maintain the soluble iron concentration in an optimal domain for cell growth. These chelating agents, called siderophores, are synthesized by bacteria and other microbes to overcome the low iron availability resulting from the minimal solubility of iron hydroxides. Siderophores selectively acquire and mediate iron transport and deposition inside the cell (Figure 1). The overall scheme of siderophore mediated iron uptake is reasonably well defined (Winkelmann 1991; Winkelmann & Carrano 1997; Sigel & Sigel 1998). However, the molecular level mechanism of many steps remains unclear, such as the nature of the specific recognition of Fe(III)-siderophore complexes by cell membrane receptors, the successive events leading to siderophore complex introduction inside the cell, and the mechanism of iron release inside the cell from its extremely stable siderophore complex. In addition, less than 10% of the total cellular iron present inside the cell is in a well defined form; the remaining quantity is present in forms poorly defined and remains to be characterized (Matzanke *et al.* 1991; Braun *et al.* 1998).

Siderophore chelation properties and the parameters affecting the stability of Fe(III)-siderophore complexes are determining factors for iron transport, as they influence iron binding, complex recognition by cell membrane receptors and iron release inside the cell. We present here a discussion of the mechanism of iron chelation and release directly related to the coordination chemistry of siderophores. The effect of ligand structure, speciation, pH and the presence of competing Fe(II) chelators on the redox potentials of iron-siderophore complexes will be addressed and a possible mechanism of iron release from a siderophore complex inside the cell through a redox process will be discussed. This presentation is largely centered on literature reports and previously unpublished data from our laboratory. Readers are directed elsewhere for a more comprehensive review of the relevant literature (Winkelmann 1991; Raymond & Telford 1995; Telford & Raymond 1996; Albrecht-Gary & Crumbliss 1998; Sigel & Sigel 1998; Albrecht-Gary & Crumbliss 1999).

Iron solubilization

The environmental aqueous chemistry of iron is largely determined by the low solubility of its hydroxide species. Under aqueous aerobic conditions iron is

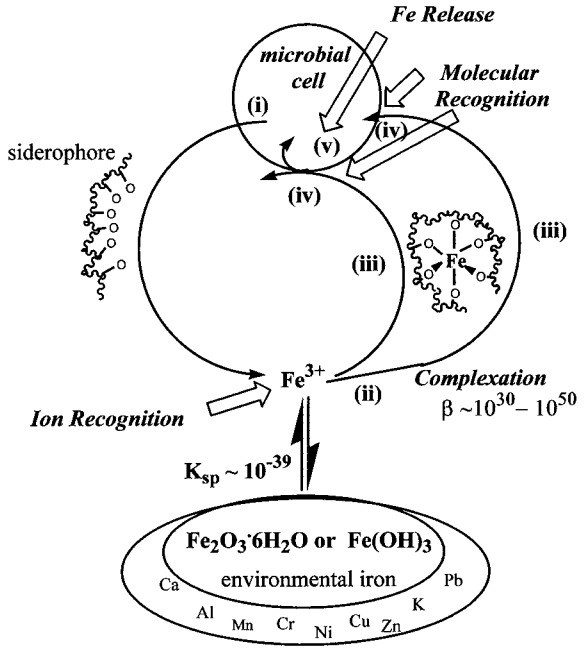

Figure 1. Schematic representation of siderophore mediated acquisition of environmental iron by microbial cells, involving: (i) siderophore ligand synthesis and release by the cell; (ii) Fe^{3+} ion recognition and complexation; (iii) diffusion to the cell surface, (iv) siderophore complex molecular recognition by cell surface receptor; (v) iron release to the cell interior

stabilized in the 3+ oxidation state. In the absence of organic or inorganic chelators the total amount of soluble iron in aqueous solution is limited by the solubility of iron hydroxide species as described in Equation 1. At pH 7.4 and in the absence of chelating ligands the total amount of soluble iron ($Fe^{3+}_{(aq)} + Fe(OH)^{2+}_{(aq)} + Fe(OH)^{+}_{2(aq)}$) is as low as 10^{-10} M.

$$Fe(OH)_{3(s)} \overset{K_{s3\text{-}i}}{\rightleftharpoons} Fe(OH)^{i+}_{3\text{-}i(aq)} + iOH^{-}_{(aq)} \quad (1)$$

In order to overcome the iron solubility problem microbes produce siderophores, which can solubilize iron hydroxides or acquire iron weakly bound to inorganic ligands or other organic chelating agents through ligand exchange reactions. In order to efficiently capture Fe(III) chelated by other ligands, siderophores must have a higher affinity for Fe(III). The solubilizing properties of siderophores can be expressed as a function of their binding affinity for Fe(III) and the pH domain according to Equations 2 and 3, where K_{sol} is

$$Fe(OH)_{3(s)} + H_ySid \overset{K_{sol}}{\rightleftharpoons} Fe\text{-}Sid + (y-3)H^+ + 3H_2O \quad (2)$$

$$\begin{aligned} Log(K_{sol}) &= LogK_{Fe-sid} + Log(K_{FeOH}) \\ &\quad -3Log(K_w) - Log(\alpha_{sid}) - 3pH \quad (3) \end{aligned}$$

the iron solubilization constant, $K_{Fe\text{-}sid}$ the overall stability constant for the iron siderophore complex, $K_{FeOH} = 10^{-38.6}$ is solubility constant for iron hydroxide, $K_w = 10^{-14}$ is the water hydrolysis constant and α_{sid} is defined as shown in Equation 4, where K_{H_nsid} are the siderophore deprotonation constants.

$$\begin{aligned} \alpha_{Sid} &= 1 + K_{Hsid}[H^+] + K_{Hsid}K_{H_2sid}[H^+]^2 \\ &\quad +\ldots + K_{Hsid}\ldots K_{H_nsid}[H^+]^n \quad (4) \end{aligned}$$

The values of K_{sol} increase as the affinity of the siderophore for iron increases. $Log(K_{sol})$ should be positive in order to effectively solubilize iron hydroxides. Representative thermodynamic data in Table 1 demonstrate that natural siderophores can efficiently solubilize iron hydroxide and consequently increase iron bioavailability. For example, desferrioxamine B and enterobactin have $log(K_{sol})$ values of 6.83 and 14.62 respectively. However, data in Table 1 are calculated by assuming saturation of the six iron coordination sites by the siderophore. Partially protonated or hydroxo containing species that can form at low or high pH regimes generally have a lower stability constant and the ability of the siderophore to solubilize iron hydroxides is decreased. Although most siderophores have K_{sol} values favoring iron solubilization, the effective *rate* of siderophore assisted iron solubilization can be very slow and will depend on the structure of the iron containing mineral and the siderophore. Recent investigations of a siderophore's ability to solubilize iron hydroxides show that they can effectively sequester iron adsorbed on different mineral oxides as well as solubilize iron hydroxides (Hersman *et al.* 1996). More detailed discussions of siderophore interactions with mineral oxides and solid surfaces are presented in the specialized literature (Hersman *et al.* 1995; Hersman 2000; Maurice *et al.* 2001).

Siderophore structure

There are almost 500 compounds identified as siderophores. Siderophores are defined as low molecular weight organic chelators with a very high and specific affinity for Fe(III). Their function is to mediate iron uptake by microbial cells. The selectivity

Table 1. Thermodynamic parameters for iron selected siderophore and synthetic siderophore complexes.

Siderophores	Log (β^{III})[a]	Log (β^{II})[b]	$E_{1/2}$ (mV) (vs NHE)	pFe[c]	Log(K_{sol})[d]	Reference
Enterobactin	49	23.91	−750	35.5	14.62	(Cooper *et al.* 1978; Percora *et al.* 1983; Lee *et al.* 1985; Loomis & Raymond 1991)
Pyoverdin	30.8	9.78	−510	27	6.97	(Albrecht-Gary *et al.* 1994)
Ferrichrome A	32.0	9.91	−440	25.2	5.45	(Anderegg *et al.* 1963; Wawrousek & McArdle 1982; 1982; Wong *et al.* 1983)
Ferrioxamine E	32.5	11.16	−477	27.7	7.87	(Anderegg *et al.* 1963; Spasojević *et al.* 1999)
Ferrioxamine B	30.6	10.29	−468	26.6	6.83	(Bickel *et al.* 1960; Schwarzenbach & Schwarzenbach 1963; Cooper *et al.* 1978; Helman & Lawrence 1989; Spasojević *et al.* 1999)
Aerobactin	22.5	4.86	−336	23.3	3.67	(Harris *et al.* 1979)
Alcaligin	64.6	22.6	−446		16.57	(Hou *et al.* 1996;
	32.3[e]	12.3[e]		23.0	8.28	Spasojević *et al.* 1999)
Rhodotorulic acid	62.3	21.1	−359		15.20	(Carrano *et al.* 1979;
	31.2[e]	10.6[e]		21.8	7.6	Spasojević *et al.* 1999)
Aceto Hydroxamic acid	28.29	11.2	−293	12.5	3.68	(Wirgau *et al.* 2002; Martell & Smith 1974, 1975, 1976, 1977, 1982, 1989)
N-methylaceto Hydroxamic acid	29.4	11.2	−348	16.2	6.87	(Spasojević *et al.* 1999; Martell & Smith 1974, 1975, 1976 1977, 1982, 1989)
L-lysine Hydroxamic acid	16.1	3.4	−214	7.1	−2.26	(Wirgau *et al.* 2002)
Tiron	46.3	>26.3	<−450	20.94		(Schwarzenbach and Willi 1951; Novicova & Novikov 1981)

[a]Overall stability constant at 25 °C for complexation of $Fe(H_2O)_6^{3+}$ by the fully deprotonated ligand; represents β_{110} for the hexadentate ligands, β_{230} for the tetradentate ligands and β_{130} for bidentate ligands.

[b]Overall stability constant at 25 °C for complexation of $Fe(H_2O)_6^{2+}$ by the fully deprotonated ligand; represents β_{110} for the hexadentate ligands, β_{230} for the tetradentate ligands and β_{130} for bidentate ligands. Calculated from Equation 11 where $E^0_{aq} = 732$ mV ($Fe(H_2O)_6^{3+}/Fe(H_2O)_6^{2+}$ couple in 1 M $HClO_4$).

[c] $-\log[\text{uncomplexed } Fe^{3+}_{aq}]$ at pH 7.4, 1 μM total Fe^{3+} and 10 μM total ligand.

[d]Calculated from Equation 3.

[e]Stability constant per Fe atom.

of siderophores for Fe(III) is achieved through optimal selection of metal binding groups, the number of binding units, and their stereochemical arrangement. Siderophores incorporate hydroxamate, catecholate and/or α-hydoxycarboxylic acid binding subunits arranged in different architectures (linear, tripodal, endocyclic or exocyclic).

Denticity is an important factor in siderophore architecture. Most siderophores are hexadentate, the optimal denticity to satisfy the six coordination sites on Fe(III). However, tetradentate siderophores are also produced by microbes to acquire Fe(III) where multimetallic assemblies may be formed to ensure full iron coordination. Data in Table 1 show an enhancement in complex stability for catecholate and hydroxamate ligands with high denticity. In addition to a denticity effect, ligand architectures which may facilitate preorganization for iron binding will also affect complex stability. Cyclic structures such as ferrioxamine E and alcaligin show a higher Fe(III) affinity compared to their linear analogues ferrioxamine B and rhodotorulic acid respectively (Figure 2; Table 1).

Ligand denticity also induces a concentration effect which favors ligands with high denticity as described by Equation 5 for a bidentate ligand (A) and

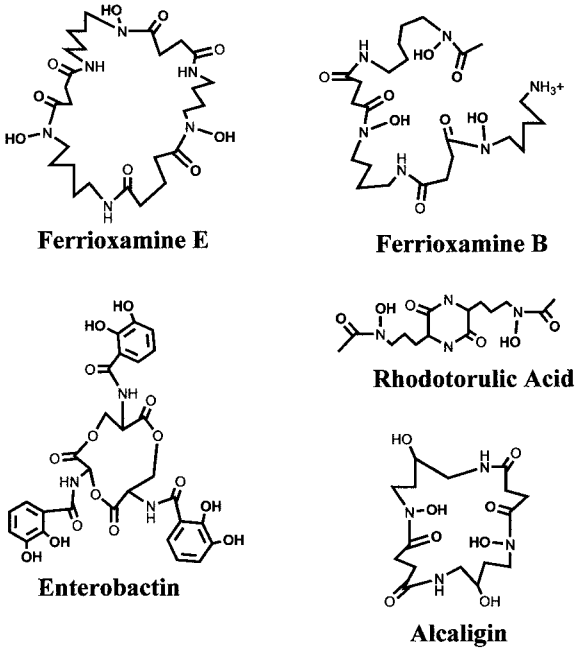

Figure 2. Representative siderophore structures with hydroxamic acid and catechol Fe(III) chelating moieties which illustrate linear, endocyclic, exocyclic, hexadentate and tetradentate architectures.

Equation 6 for a hexadentate ligand (L).

$$[A^-] = \left\{ \frac{[FeA_3]}{[Fe^{3+}_{aq}]\beta_{130}} \right\}^{1/3} \quad (5)$$

$$[L^{3-}] = \left\{ \frac{[FeL]}{[Fe^{3+}_{aq}]\beta_{110}} \right\} \quad (6)$$

The concentration effect can be illustrated by comparing the free ligand concentration required to establish a given ratio between the complexed and free iron in solution. For example, the bidentate acetohydroxamic acid concentration (log $\beta_{130} = 28.4$ in Equation 5) (Martell & Smith 1974, 1975, 1976, 1982, 1989) needs to be 10^{18} higher than ferrioxamine B (log $\beta_{110} = 30.6$ in Equation 6) (Schwarzenbach & Schwarzenbach 1963) to achieve a 10^3/l ratio between the complexed and uncomplexed form of Fe(III) (Albrecht-Gary & Crumbliss 1998).

Hexadentate siderophores

Most hexadentate siderophores are based on hydroxamate and/or catecholate binding subunits and have a very high affinity for Fe(III), discriminating against Fe(II). Desferrioxamine B (Figure 2) with three hydroxamate units achieves full iron coordination (Dhungana *et al.* 2001). Its affinity for Fe(III) is log $\beta^{\mathrm{Fe(III)}}_{110} = 30.6$ (Schwarzenbach & Schwarzenbach 1963), which is 20 orders of magnitude higher than for Fe(II) (log $\beta^{\mathrm{Fe(II)}}_{110} = 10.0$) (Cooper *et al.* 1978; Helman & Lawrence 1989; Spasojević *et al.* 1999). The affinity of desferrioxamine E for Fe(III) is two orders of magnitude higher than desferrioxamine B (Log $\beta^{Fe(III)}_{110} = 32.5$ (Anderegg *et al.* 1963; Konetschny-Rapp *et al.* 1992) and it also has a lower binding affinity for Fe(II) (log $\beta^{\mathrm{Fe(II)}}_{110} = 12.1$) (Spasojević *et al.* 1999). The increase in the stability constant of Fe(III)-desferrioxamine E over Fe(III)-desferrioxamine B is attributed to a macrocycle effect resulting from ligand preorganisation for iron binding in the case of ferrioxamine E (Figure 2).

Hexadentate siderophores have a much higher affinity toward Fe(III) binding than their bidentate analogues. Both ligands form fully coordinated Fe(III) complexes at neutral pH and their log $\beta^{\mathrm{Fe(III)}}$ values are relatively similar (for example: log $\beta^{\mathrm{Fe(III)}}_{110} = 30.6$ for ferrioxamine B and log $\beta^{\mathrm{Fe(III)}}_{130} = 28.29$ for N-methyl acetohydroxamic acid; Table 1). However, since log β values describe equilibria with the fully deprotonated siderophore, comparison of these values does not take into account competition from H^+ arising from the pH of the medium. Furthermore, since β values are based on concentration measurements, the units for different denticities vary and therefore are not directly comparable. Consequently, direct comparison of these β values does not assess the difference in these ligands' respective affinity for Fe(III) at ambient conditions. Comparison of pFe values (-log[uncomplexed Fe^{3+}_{aq}] at pH 7.4, 1 μM total Fe^{3+} and 10 μM total ligand) gives a better evaluation of the differences in ligand affinity for iron (Raymond *et al.* 1984). Ferrioxamine B with a pFe value of 26.6 has a much higher affinity for iron compared to N-methylacetohydroxamic acid, with a pFe value of 16.2 (Table 1). An enhancement in the binding affinity is also observed for catecholate as we compare hexadentate enterobactin with a pFe value of 35 to a simple bidentate catecholate ligand like tiron with a pFe value of 20.9 (Table 1). In general hexadentate siderophores have a much higher affinity for Fe(III) compared to tetradentate siderophores, which have a higher iron affinity compared to bidentate siderophores (Table 1) (Albrecht-Gary & Crumbliss 1998).

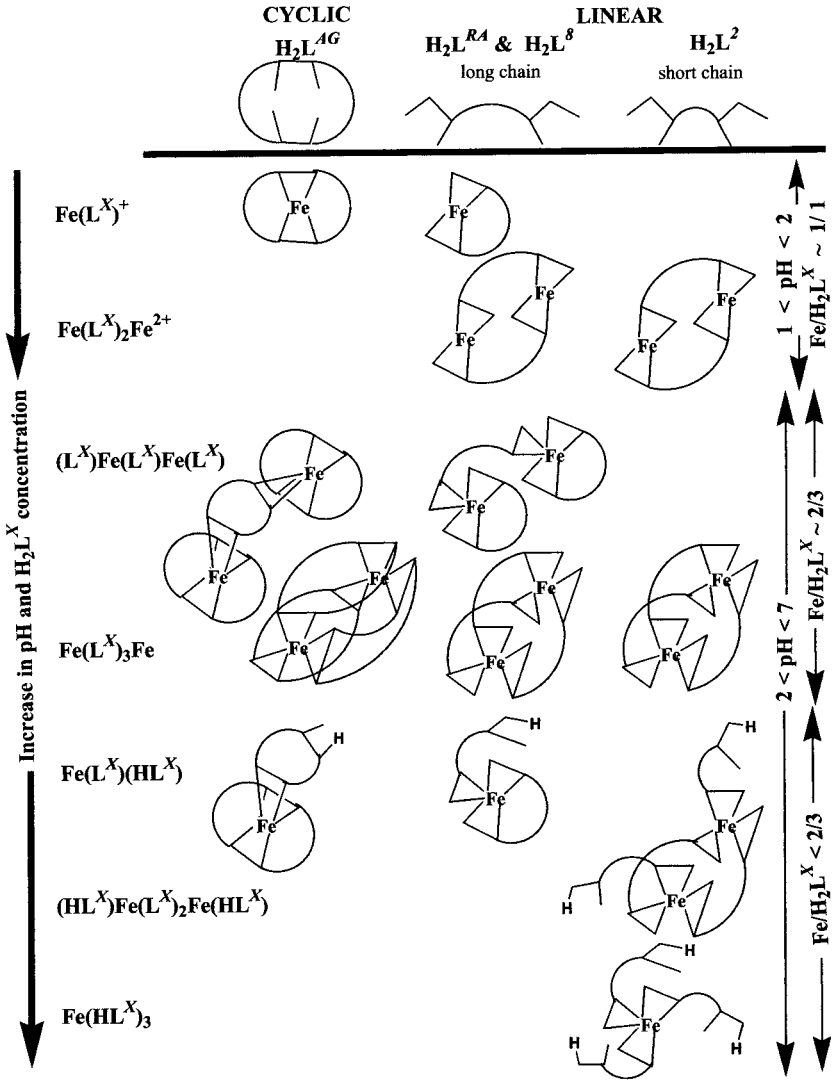

Figure 3. Speciation of tetradentate di-hydroxamic acid complexes of Fe(III) present in aqueous solution at variable Fe(III)/ligand ratios and pH as determined by electrospray ionization mass spectrometry. Examples of cyclic and linear ligand architectures are presented (coordinated H_2O not shown in figure): alcaligin (H_2L^{AG}); rhodotorulic acid (H_2L^{RA}); $CH_3N(OH)C(O)(CH_2)_8C(O)N(OH)CH_3$ (H_2L^8); $CH_3N(OH)C(O)(CH_2)_2C(O)N(OH)CH_3$ (H_2L^2). Figure adapted from (Spasojević *et al.* 2001) and used with permission

Tetradentate siderophores

This class of siderophores differs from their hexadentate analogues since a single molecule cannot achieve full Fe(III) coordination saturation. Rather, two or three molecules of the ligand (H_2L) assemble to satisfy the six iron coordination sites, giving species of variable stoichiometry (e.g., Fe_2L_3, $FeL(LH)$, $Fe(LH)_3$, $FeL(OH_2)_2^+$, $Fe_2L_2(OH_2)_4^{2+}$, etc) depending on the ligand architecture, metal to ligand ratio and the pH domain (Figure 3) (Spasojević *et al.* 2001). The best characterized tetradentate siderophores are alcaligin and rhodotorulic acid (Figure 2). In 1:1 ligand to iron ratio, alcaligin, a cyclic siderophore, unambiguously forms a monomeric complex, $FeL^{AG}(H_2O)_2^+$ (Spasojević *et al.* 2001). The alcaligin ligand is preorganized to form monomeric complexes, as demonstrated by X-ray crystal structures of the iron-free ligand and its complex (Hou *et al.* 1996, 1998). The linear structure of rhodotorulic acid is suitable for the formation of both monomeric and dimeric complexes with Fe(III). An electrospray ionization mass spectroscopy investigation of rhodotorulic acid complexes showed that in 1:1 metal to ligand ratio the complex

is exclusively monomeric (Caudle *et al.* 1994b; Spasojević *et al.* 2001). The amide ring separating the two hydroxamate units doesn't add sufficient strain to induce Fe(III) complex dimerization. Synthetic analogues of the linear rhodotorulic acid siderophore show that the distance between the hydroxamate units should be shorter than six carbons to induce Fe(III) complex dimerization (Caudle *et al.* 1994a, b; Spasojević *et al.* 2001). The favored monomeric structure of these tetradentate siderophores disfavors the formation of di-iron complexes that could potentially act as redox catalysts in the production of reactive oxygen species. Tetradentate siderophores form complexes of the stoichiometry Fe_2L_3 at neutral pH and optimal ligand to metal ratio. However, when the ligand is present in excess over iron, assemblies of the stochiometry Fe(L)(LH) and $Fe(LH)_3$ are also formed (Figure 3). Tetradentate siderophores exhibit the same selectivity for Fe(III) over Fe(II) as their hexadentate analogues (Spasojević *et al.* 1999).

Cell receptor recognition

The low bioavailability of iron caused by the insolubility of iron hydroxides prevents the cell from acquiring Fe(III) through diffusion to the cell interior via porins. Due to their hydrophilic character, Fe(III)-siderophore complexes cannot be transported through the cell membrane by a simple diffusion process, and consequently receptors are involved. In gram negative bacteria the Fe(III)-siderophore complex is first captured at the cell surface by specific protein receptors, followed by transport to the periplasmic space facilitated by the proton motive force of the periplasmic space and an energy transduction provided by a functional Ton system (Kadner 1990; Bradbeer 1993; Postle 1993; Larsen *et al.* 1996; Stojiljkovic & Sirinivasin 1997; Braun 1998; Braun *et al.* 1998; van der Helm 1998). The details of iron-siderophore complex recognition by membrane receptors is still an open question, but in some cases data are available which demonstrate that ligand donor atom configuration around the metal is important (Raymond & Carrano, 1979; Ferguson *et al.* 1998; Clarke *et al.* 2000).

X-ray crystal structures of *E. coli* outer membrane ferric siderophore receptors have recently been reported for FhuA, a ferrichrome receptor, and FepA, an enterobactin receptor (Ferguson *et al.* 1998; Locher *et al.* 1998; Buchanan *et al.* 1999). These structures show two distinct receptor domains, a β-barrel and a N-terminal globular domain that serves as a 'plug' for the barrel, thus dividing the receptor into an outer and inner compartment. The siderophore complex in these receptors is apparently recognized by being bound in the outer chamber through a combination of H-bonding and van der Waals contacts. These interactions involve oxygen groups coordinating iron and also carbonyl groups from the amide group present in the siderophore backbone. A crystal structure is also available for FhuD, an *E. coli* periplasmic binding protein which recognizes several ferric hydroxamate siderophores, including ferrichrome and ferrioxamine B (Clarke *et al.* 2000). Selected aspects of receptor molecular recognition are modeled in our laboratory for ferrioxamine B via second coordination shell host-guest interactions and the formation of ionophore-siderophore assemblies (Caldwell & Crumbliss 1998; Spasojević & Crumbliss 1998, 1999; Trzaska *et al.* 2000, 2001).

Recent investigations of receptor mediated membrane iron transport illustrate the complexity of the overall process and the apparent significance of recognition and binding of an iron-free siderophore to the receptor. Schalk and co-workers found that the outer membrane receptor FpvA in *Pseudomonas aeruginosa* binds iron-free pyoverdin and that membrane iron transport involves displacement of the apo-siderophore by the Fe(III)-siderophore (Schalk *et al.* 1999, 2001, 2002). Raymond and co-workers describe a shuttle mechanism for membrane iron transport in *Aeromonas hydrophila* (Stintzi *et al.* 2000). Evidence is given which demonstrates Fe(III) exchange between a number of siderophore carriers and an outer membrane receptor bound apo-siderophore, followed by a receptor conformational change and transport of the iron-siderophore complex into the cell. Its not yet clear whether all membrane receptors bind the apo-siderophore and if so what is the relevance of the assembly formed. However, these results demonstrate the complexity of the cell membrane recognition/transport process and the fact that the kinetics of Fe(III)/ligand exchange or Fe(III) siderophore/apo-siderophore-receptor assembly exchange processes are important (Dhungana & Crumbliss 2001).

Ligand exchange kinetics

Once the siderophore complex is recognized at the cell surface, the iron must eventually escape from the chemical environment of the siderophore ligand.

These ligand exchange reactions are usually slow at *in vitro* conditions due to the very high binding affinity and selectivity of siderophores toward Fe(III), which ensures the *in vivo* acquisition of iron even when its concentration is very low. Investigations of the kinetics and the mechanism of iron reactivity in solution cover a wide range of topics, such as the reactivity of the hexaaqua ($Fe(H_2O)_6^{3+}$) and hydroxide ($Fe(H_2O)_5(OH)^{2+}$) species, iron binding to organic and inorganic ligands, and ligand exchange between iron complexes (Biruš *et al.* 1993; Albrecht-Gary & Crumbliss 1998). Kinetic examination of H^+ assisted iron release from siderophore complexes provides data necessary to formulate mechanisms by which these assemblies form and dissociate. The first step in the dissociation of iron siderophore complexes normally involves the dissociation of a bidentate moiety (e.g., hydroxamate or catecholate) from the fully chelated iron, which is relatively fast as a proton driven reaction at low pH; $t_{1/2} \cong$ 2–5 ms (Monzyk & Crumbliss 1982; Biruš *et al.* 1987; Boukhalfa *et al.* 2000; Boukhalfa & Crumbliss 2000). This step represents the replacement of one binding unit from the first coordination shell of Fe(III) by water ligands. The lability of the fully coordinated iron is an important factor in iron release and exchange. Through the complex dechelation process, vacant coordination sites on iron become available, which further lowers the binding affinity of the siderophore to iron and permits the formation of ternary complexes which may facilitate further dissociation of the siderophore complex (Boukhalfa *et al.* 2000; Boukhalfa & Crumbliss 2000, 2001).

Ferrioxamine B and ferrioxamine E ligand dissociation kinetics

Ferrioxamines B and E (Figure 2) undergo proton driven dissociation kinetics through a single path involving successive dechelation reactions (Monzyk & Crumbliss 1982; Biruš *et al.* 1987; Spasojević & Crumbliss 2002). The first step in the dissociation process involves a change in iron coordination from hexacoordination to tetracoordination. The proton assisted dissociation of one hydroxamate group from the fully coordinated ferrioxamine B complex is relatively fast, $k_1 = 3.8 \times 10^2\ M^{-1}\ s^{-1}$ (Monzyk & Crumbliss 1982; Biruš *et al.* 1987). The resulting complex has two coordination sites occupied by two H_2O ligands. The further dissociation of the complex is much slower; a subsequent proton driven step having a second order rate constant $k_3 = 2.3 \times 10^{-2}\ M^{-1}\ s^{-1}$. The contrast between k_3 and k_1 demonstrates the high lability for the hexacoordinated complex compared to the tetracoordinated analogue. The dissociation occurs as a single series of sequential steps involving the dissociation of each hydroxamate unit. Further dissociation of the bidentate complex leads to complete Fe(III) release from the siderophore. The final step in ligand dissociation has a rate constant $k_4 = 5 \times 10^{-4}\ M^{-1}\ s^{-1}$ which is much smaller compared with the two preceding steps. This final dissociation of the ferrioxamine complex is the result of a bidentate mono-hydroxamic acid dissociation which follows a parallel path leading to the formation of hexaaqua iron, $Fe(H_2O)_6^{3+}$ and iron hydroxide, $Fe(H_2O)_5(OH)^{2+}$ (Monzyk & Crumbliss 1982; Biruš *et al.* 1987).

Tetradentate ligand dissociation kinetics

Ligand dissociation from tetradentate siderophores changes drastically compared to hexadentate siderophores as a result of a change in the structure of the complex and its lability. In contrast with hexadentate siderophores, tetradentate siderophores undergo multiple path dissociation mechanisms involving different complex intermediates (Boukhalfa & Crumbliss 2000). The nature of these intermediates and the dissociation path involved is dependent on the siderophore complex and the pH domain. The first step in the proton driven dissociation of the tris(hydroxamato)iron(III) complex of alcaligin ($k_3 = 1.5 \times 10^2\ M^{-1}\ s^{-1}$) and rhodotorullic acid ($k_3 = 6.8 \times 10^2\ M^{-1}\ s^{-1}$) (Boukhalfa *et al.* 2000) at 25 °C is relatively fast, making these complexes very labile and comparable to the dissociation rate observed for hexadentate siderophores (Monzyk & Crumbliss 1982, Biruš *et al.* 1987; Boukhalfa *et al.* 2000). The resulting tetracoordinated complex is relatively stable; the ligand dissociation in the following step needs a drop in the pH at *in vitro* conditions to <1! Iron dissociation from the alcaligin complex $Fe(L^{AG})H_2O)_2^+$ is extremely sluggish and proceeds through ligand decomposition. Although tetracoordinated Fe(III)-rhodotorulic acid ($Fe(L^{RA})(H_2O)_2^+$) dissociation is much more labile compared to alcaligin, the kinetics remains slow and proceeds only at a very acidic pH. However, the ligand dissociation kinetics and exchange can be catalyzed by the presence of Cl^- ion in solution (Boukhalfa & Crumbliss 2001). Environmental chloride ion binding to iron enhances lig-

and exchange by increasing the ligand electron donor capabilities in the first coordination sphere of Fe(III).

Redox facilitated ligand exchange

The stability constants of ferric siderophores are among the highest measured for iron complexes. The high stability of these complexes makes ligand exchange and iron release thermodynamically unfavorable and slow. As discussed above, high $[H^+]$ is required for Fe(III)-siderophore dechelation, and even when complex dissociation occurs in acidic pH the rate of complete ligand dissociation remains relatively slow (Boukhalfa *et al.* 2000). However, partial dechelation of the complex to give open coordination sites can be relatively fast as noted above. The presence of free coordination sites on the iron center decreases the Fe(III) binding constant of the siderophore and facilitates the formation of ternary complexes. The formation of ternary complexes is the first step in a facilitated ligand exchanges process. This exchange process may be further enhanced through the reduction of ferric siderophore complexes to the corresponding ferrous complexes. This assumes the presence of agents able to reduce the ferric iron siderophore complex to the ferrous form.

The redox potentials observed for most siderophores are in the range from −350 mV to −750 mV/NHE (Table 1), which places them out of the range of most biological reducing agents like NADPH or NADH (E = −320 mV/NHE). The very negative redox potentials found for siderophores is the underlying reason for the significant difference between their affinity for Fe(III) and Fe(II) (Table 1). The difference in siderophore affinity for ferric and ferrous iron is related to the difference in Fe(III) and Fe(II) Lewis acid character that determines the interaction between the ligand donor groups and the metal center. The fully hydrated form of iron ($Fe(H_2O)_6^{3+}$) undergoes Fe(III/II) redox cycling at +770 mV/NHE. As a strong Lewis acid, ferric ion prefers hexacoordination provided by hard donor groups like oxygen containing anions. In contrast, ferrous iron is a soft or borderline soft metal center having more affinity toward polarizable ligands often incorporating nitrogen donor groups. The redox potential of stable Fe(II) complexes is usually shifted to more positive values relative to the aquo ion.

Scheme 1 illustrates the reversible chelation and redox processes involving the formation of the siderophore complex and the redox equilibrium between the two oxidation states of the iron-siderophore complex. Equation 11, which may be derived from this scheme, illustrates that the siderophore redox potential is determined by the difference in the siderophore binding affinity for Fe(III) and Fe(II), where E^0_{aq} is

Scheme 1

$$Fe^{III} + Sid \xrightleftharpoons{\beta_{110}^{Fe(III)}} Fe^{III}Sid \quad (7)$$

$$\downarrow e^- E_{Fe^{III/II}} \qquad \downarrow e^- E_{Fe^{III/II}Sid} \quad (8)\ (9)$$

$$Fe^{II} + Sid \xrightleftharpoons{\beta_{110}^{Fe(II)}} Fe^{II}Sid \quad (10)$$

$$E_{Fe^{III/II}Sid} = E^0_{aq} - 59.15Log\left(\frac{\beta_{110}^{Fe(III)}}{\beta_{110}^{Fe(II)}}\right) \quad (11)$$

the redox potential for the hexaaquated iron (E^0_{aq} = +770 mV/NHE), and $\beta_{110}^{Fe(III)}$ and $\beta_{110}^{Fe(II)}$ are the siderophore overall stability constants for Fe(III) and Fe(II) chelation, respectively. Equation 11 may be used to calculate the $\beta_{110}^{Fe(II)}$ values that are listed in Table 1. Equation 11 shows that an increase in the Fe(III)-siderophore stability constant relative to the Fe(II)-siderophore stability constant results in a decrease of the redox potential to more negative values. *This also illustrates that the negative redox potential for the siderophores may be a requirement for the selectively of the siderophore chelator for Fe(III), since most of the competing ions present in the environment are in the +2 oxidation state.*

Siderophores will facilitate environmental Fe(II) oxidation in the presence of O_2. This is evident from the strongly negative redox potentials for Fe(III)-siderophores and from Equation 11 which illustrates that in the presence of O_2, a Fe(II)-siderophore will be readily oxidized to a Fe(III)-siderophore.

Parameters like pH, ligand denticity, and the presence of competing chelators can be very effective in shifting the redox potential of iron-siderophore complexes into the domain where the complex becomes accessible to biological reducing agents. A discussion of some of these factors follows.

pH effect on the redox potential of iron siderophore complexes

The strong dependence of Fe(III)-siderophore redox potentials on the pH is directly related to

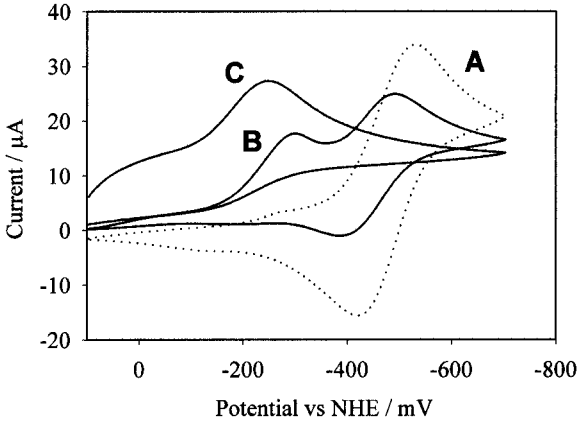

Figure 4. Cyclic voltammograms of ferrioxamine B in aqueous solution as a function of pH: A, pH>4; B, 3<pH<4; C, pH<2.5. Conditions: Glassy carbon working electrode of 0.02 cm^2 surface area, Ag/AgCl reference electrode, Pt auxiliary electrode, $\nu = 60$ mV/s, T = 25 °C, [ferrioxamine B] = 5 mM, $I = 100$ mM ($NaClO_4/HClO_4$), pH adjusted by addition of NaOH or $HClO_4$.

the pH dependence of their stability. Since all siderophores and their iron complexes undergo protonation/deprotonation reactions, the redox potential measured is strongly dependent on the pH domain examined. The model described in Equations 7–11 considers the ligation and redox equilibria involving the fully deprotonated siderophore and the hexacoordinated iron complex. However, in the pH ranges where the complex is present in solution as a mixture of different protonated species the formal redox potential is expressed as a function of the concentrations of different species present at that pH. As a result of the lower stability of the protonated Fe(II)-siderophore complexes that dissociate rapidly, qualitative consideration of the equilibrium requirements of the Nernst equation (Equation 12) shows that the effective solution potential at which the Fe(III)-siderophore is reduced occurs at a more positive potential when

$$E^f = E^0_{Fe^{III/II}Sid} - 59.15Log\left(\frac{[Fe^{III}Sid]}{[Fe^{II}Sid]}\right) \qquad (12)$$

protonation occurs. That is, at a given solution potential E, as [Fe^{II}Sid] decreases due to proton driven dissociation, more Fe^{III}Sid is reduced. The net result is that protonation of the siderophore ligand facilitates ligand dissociation and shifts the redox potential into a region where the complex is more easily reduced.

Representative cyclic voltammograms of ferrioxamine B obtained at different pH values are shown in Figure 4 (Boukhalfa & Crumbliss). The data indicate a reversible electrochemical process above pH 4 where $E_{1/2} = -483$ mV/NHE. The reversible one-electron wave observed is attributed to the fully hexacoordinated ferrioxamine B complex, the only species present over the pH range 4 to 10. As the pH is lowered to more acidic values a second irreversible redox process is observed with a reduction wave situated at −280 mV/NHE. The presence of this second wave is attributed to the reduction of a protonated ferrioxamine B complex. Below ca pH 2.5 the reversible process is no longer observed and the irreversible reduction wave is observed at E = −230 mV/NHE. Under acidic conditions (pH < 4) most Fe(III)-siderophore complexes show an irreversible one-electron wave in cyclic voltammogram experiments. The loss of reversibility is generally attributed to the low stability of protonated Fe(II)-siderophore complexes that dissociate readily after the reduction of the corresponding Fe(III)-siderophore complex. The pH dependence of ferrioxamine B cyclic voltammetry is illustrated in Scheme 2. The redox wave at −230 mV is tentatively

Scheme 2

$$FeSid + H^+ \overset{K_{FeHSid}}{\rightleftharpoons} FeHSid(H_2O)_2 \qquad (13)$$

$$Fe^{III}Sid + e- \rightleftharpoons Fe^{II}Sid \qquad (14)$$

$$Fe^{II}Sid + 3H^+ \rightleftharpoons Fe^{2+}_{aq} + H_3Sid \qquad (15)$$

attributed to the tetracoordinated ferrioxamine B complex, Fe(H_2DFB) $(OH_2)^{2+}_2$, formed in Equation 13.

Model Equation 16 was derived to quantitatively account for the pH dependence of the redox potential of the ferrioxamine B complex, where $K_{Fe^{II}Hsid}$ is defined as in Equation 17.

$$E^f = E^0_{Fe^{III}Sid} + \frac{RT}{nF}Log(1 + K_{Fe^{II}HSid}[H^+]) \qquad (16)$$

$$K_{Fe^{II}HSid} = \frac{[Fe^{II}HSid]}{[Fe^{II}Sid][H^+]} \qquad (17)$$

The formal redox potential of ferrioxamine B increases as the pH progresses to more acidic values. The protonation constants for the Fe(II)-siderophore complexes can be determined by numerical fitting of Equation 16 to the experimental variation of the formal redox potentials as a function of pH. When the pH is situated in a range where multiple protonated species of the ferrous and ferric complex are simultaneously

present in solution the redox potential is related to pH through Equation 18, where $K_{Fe^{II}H_nSid}$ and $K_{Fe^{III}H_nSid}$

$$E^{f} = E^{0}_{Fe^{III}Sid} + \frac{RT}{nF}Log(1 + K_{Fe^{II}HSid}[H^+] + ... + K_{Fe^{II}HSid}...K_{Fe^{II}H_nSid}[H^+]^n) - \frac{RT}{nF}Log(1 + K_{Fe^{III}HSid}[H^+] + ... + K_{Fe^{III}HSid}...K_{Fe^{III}H_nSid}[H^+]^n) \quad (18)$$

are the different protonation constants for the Fe(II) and Fe(III)-siderophore complexes present in the experimental pH range.

The key points presented here which are relevant to siderophore mediated iron transport are that for siderophore complexes for which Fe(II)-siderophore complexes may become protonated at higher pH than Fe(III)-siderophore complexes, the formal redox potential for the complex will be positively shifted (the Fe(III) center will be more easily reduced) with increasing $[H^+]$. Regions of increased $[H^+]$ in patches on the cell surface and/or intracellular compartments will certainly facilitate reductive dissociation of iron from its siderophore complex. A further positive shift in siderophore redox potential comes into play as a result of significant dissociation of the Fe(II)-siderophore complex upon reduction.

Consequently, while a significantly negative thermodynamic redox potential for Fe-siderophore complexes is a necessary manifestation of the high degree of selectivity of the siderophore ligand for environmental Fe(III) ions (Equation 11), this negative thermodynamic potential does not eliminate from consideration the reductive release of iron from the siderophore complex through reduction by biological reducing agents such as NADH.

Ligand denticity effect on the redox potentials of iron siderophore complexes

Just as the ligand denticity and architecture affects the stability of iron complexes, they also influence their redox potentials. The plot in Figure 5 illustrates a linear dependence of the redox potential as a function of pFe values for a number of iron-hydroxamate complexes (Spasojević *et al.* 1999; Dhungana *et al.* 2002; Wirgau *et al.* 2002). An increase in ligand denticity enhances complex stability, which results in higher pFe values. The increase in Fe(III) complex stability results in stabilization of the Fe(III) complexes over their Fe(II) form, which results in a much more negative redox potential (Equation 11). The data in

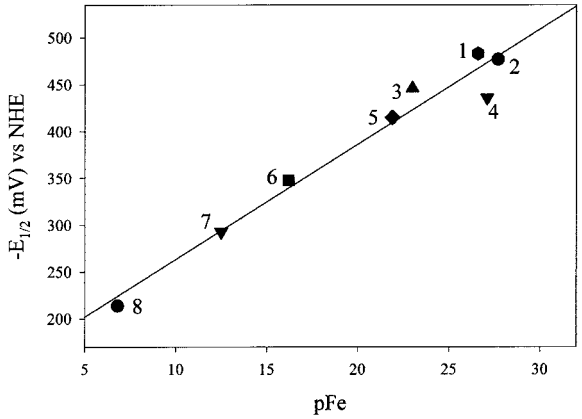

Figure 5. Plot of reversible redox potential ($-E_{1/2}$) as a function of pFe for the fully coordinated Fe(III) complexes of natural and synthetic hydroxamic acid siderophores. 1, ferrioxamine B; 2, ferrioxamine E. 3, alcaligin; 4, saccharide-trihydroxamic acid; 5, rhodotorulic acid; 6, N-methylacetohydroxamic acid; 7, acetohydroxamic acid; 8, L-lysinehydroxamic acid. Data taken from (Spasojević *et al.* 1999; Dhungana *et al.* 2002; Wirgau *et al.* 2002).

Figure 5 show a strong denticity effect on the redox potential; hexadentate siderophores with the highest stability possess the most negative redox potentials. As the denticity decreases to tetradentate and bidentate the stability of the Fe(III)-siderophore complexes drops also, which results in more positive redox potentials. This suggests a more facile *in vivo* removal of iron from lower denticity siderophores *via* a reductive process. This may also suggest a reason for the organism to expend the necessary energy to hydrolyze a siderophore chelate backbone to reduce its denticity subsequent to intracellular incorporation.

Iron(II) chelator effect on the redox potentials of iron siderophore complexes

Subsequent to reduction (Equation 19), the Fe(II)-siderophore complex can in principle release iron to a competing chelator (L) with a high affinity for Fe^{2+}_{aq} through a ligand exchange reaction (Equation 20). The magnitude of the exchange reaction is characterized by the exchange constant K_{ex}, calculated as the ratio between the stability constants ($K_{Fe^{II}sid}$ and $K_{Fe^{II}L}$) of the Fe(II) complexes for the two competing ligands (Equation 21). When the affinity of the competing ligand L toward Fe^{2+}_{aq} is higher than the siderophore's affinity for ferrous iron, the exchange reaction is displaced toward the dissociation of the Fe(II)-siderophore complex. (This effect can also be achieved through a high ambient [L]/[Sid] ratio.) In such conditions the ratio between the Fe(III)-

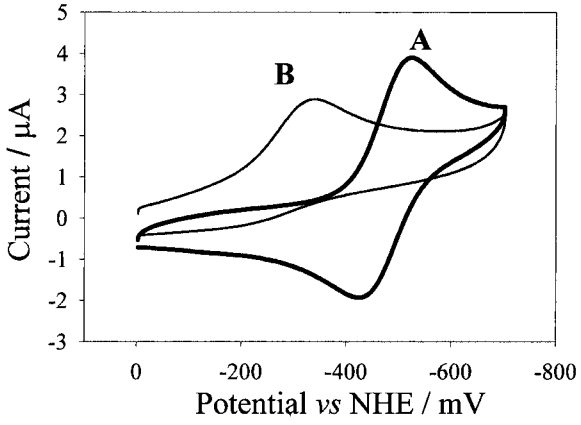

Figure 6. Cyclic voltammograms of ferrioxamine B in aqueous solution (A) and in the presence of 1,10-phenanthroline (B). Conditions: Glassy carbon working electrode of 0.02 cm^2 surface area, Ag/AgCl reference electrode, Pt auxiliary electrode, $\nu = 70$ mV/s, T = 25 °C. A: [ferrioxamine B] = 0.6 mM, pH 5.25, aqueous solution $I = 200$ mM (NaCl). B. [ferrioxamine B] = 0.6 mM, pH 6.88, aqueous solution with H_2O/DMF = 80%/20% and $I = 200$ mM (NaCl).

siderophore complex and the reduced form (Fe(II)-siderophore) changes. These changes directly affect the effective redox potential of the Fe(III)-siderophore complex. The formal redox potential is related to the siderophore pH dependent redox potential ($E_{Fe^{III}Sid}$) and the competing ligand's (L) affinity for Fe(II) through Equation 22, where $E_{Fe^{III}Sid}$ is equivalent to E^f in Equation 18.

$$Fe^{III}Sid + e^- \rightleftharpoons Fe^{II}Sid \qquad E^0_{Fe^{III}Sid} \tag{19}$$

$$Fe^{II}Sid + L \rightleftharpoons Fe^{II}L + Sid \quad K_{ex} \tag{20}$$

$$K_{ex} = \frac{K_{Fe^{II}L}}{K_{Fe^{II}Sid}} = \frac{[Fe^{II}L][Sid]}{[Fe^{II}Sid][L]} \tag{21}$$

$$E^f = E_{Fe^{III}Sid} + 59.15Log(1 + K_{ex}\frac{[L]}{[Sid]}) \tag{22}$$

The model in Equation 22 is reduced to Equation 18 in the absence of competing ligands where the formal redox potential is expressed as function of pH. However, in the presence of a ligand L with a high affinity for Fe(II) the formal redox potential is shifted to a more positive potential domain where the complex is easier to reduce.

To illustrate the effect of an Fe(II) chelator on the potential at which an Fe(III)-siderophore may be reduced, we present the cyclic voltammogram of ferrioxamine B at pH 7 in the presence of phenanthroline (an effective Fe(II) chelator) in Figure 6

Scheme 3

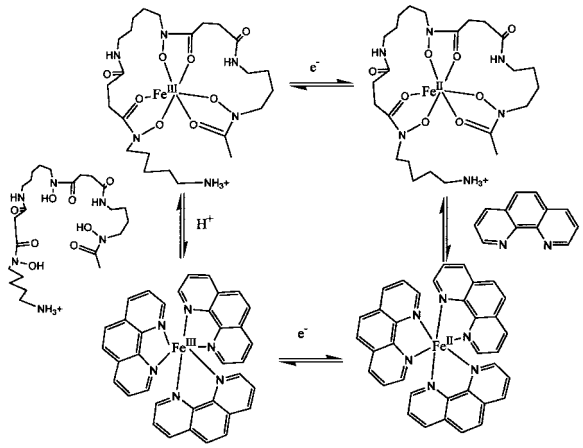

(Boukhalfa & Crumbliss). In the absence of phenanthroline the Fe(III/II)-ferrioxamine B redox couple exhibits a reversible voltammogram giving $E_{1/2} = -483$ mV/NHE. However, in the presence of excess phenanthroline the reduction wave is significantly shifted to more positive values and the redox couple becomes irreversible. The loss of reversibility is attributed to the exchange reaction occurring between the free phenanthroline and Fe(II)-ferrioxamine B as illustrated in Scheme 3. Competition between the siderophore and Fe(II) chelator generally results in poor reversibility of the cyclic voltammogram. The low stability of Fe(II)-siderophore complexes and their rapid dissociation kinetics are normally the predominant parameters inducing this poor reversibility.

Conclusions and perspectives

In this mini review we have analyzed aspects of the coordination chemistry of the iron siderophore complexes that are pertinent to microbial iron acquisition. We first demonstrated that solubilization of environmental iron is an important initial step in this process and that its efficiency is related to the thermodynamic Fe(III) binding constant (β) for the siderophore. Ligand architecture and denticity play an important role in determining the affinity of a siderophore for Fe(III). From the perspective of thermodynamic binding constants, hexadentate ligands are optimum siderophore structures. We demonstrated that ambient concentrations of tetradentate siderophores required to fully coordinate Fe(III) are several orders of magnitude

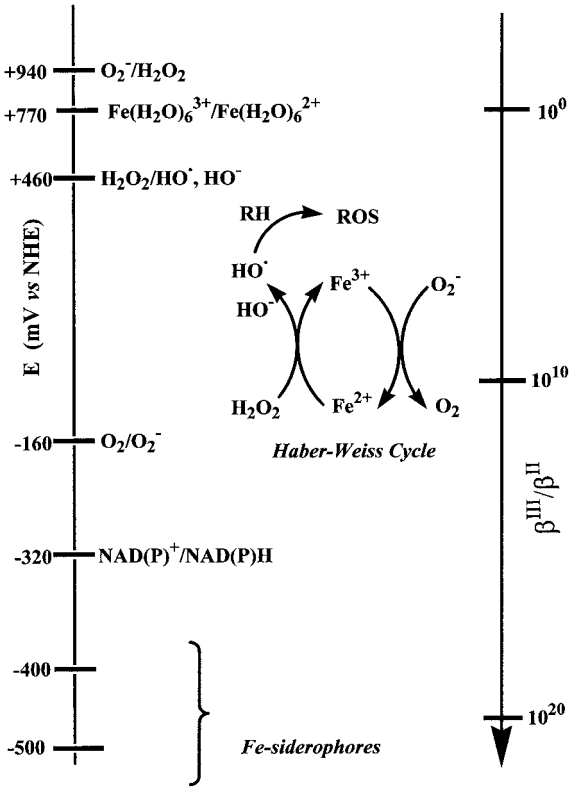

Figure 7. Chart showing the negative range of redox potentials (E vs NHE) for the Fe(III) siderophores relative to other benchmark biological redox potentials (left vertical bar) and the variation in ratio of Fe(III)-siderophore/Fe(II)siderophore stability constants ($\beta^{III}/(\beta^{II}$; right vertical bar) with changing redox potential according to Equation (11).

higher than that required for hexadentate siderophores. Consequently, one may justifiably ask: '*Why in the course of evolution are tetradentate siderophores utilized?'* We suggest that there may be two reasons, which are related to ligand lability and Fe(III/II) redox. We have shown that tetradentate siderophores (H_2L) chelate Fe(III) to form a variety of species (e.g., Fe_2L_3, $FeL(H_2O)_2^{z+}$, $Fe(L)(HL)^{z+}$, FeL_3^{z+}) which are labile with respect to ligand exchange (Boukhalfa *et al.* 2000; Boukhalfa & Crumbliss 2000), an important process in the intracellular release of iron. Furthermore, tetradentate coordination provides labile aquated coordination sites on iron ($FeL(H_2O)_2^{z+}$) which may facilitate molecular recognition and/or iron release through a catalytic mechanism involving ternary complex formation with environmental ions such as Cl^- (Boukhalfa & Crumbliss 2001). Tetradentate siderophore complexes of Fe(III) are also thermodynamically easier to reduce than their hexadentate counterparts (Figure 5), leading to rapid dissociation of Fe(II).

While high siderophore complex stability constants provide a chemical basis for iron selectivity and solubilization by siderophores, this presents a problem with respect to iron dissociation and incorporation into the cell. We have demonstrated that proton driven ligand exchange reactions, particularly for hexadentate siderophores, are often slow and require pH ranges beyond that found at the cellular level. As noted above, tetradentate siderophores have a potential advantage here. Another mechanism for iron release presented here is redox facilitated ligand exchange. Fe_{aq}^{2+} is a more labile ion than Fe_{aq}^{3+} (e.g., the $t_{1/2}$ for bound water in $Fe(H_2O)_6^{2+}$ is 10^4 shorter than in $Fe(H_2O)_6^{3+}$) (Ducommun *et al.* 1980; Dodgen *et al.* 1981; Grand & Jordan 1981; Swaddle & Merbach 1981; Lincoln & Merbach 1995). As we note in Table 1, Fe(II)-siderophore complexes are some 20 orders of magnitude less stable than their Fe(III) counterparts. Consequently, on both thermodynamic and kinetic considerations, reduction of an Fe(III)-siderophore complex followed by ligand exchange appears to be a viable *in vivo* mechanism for Fe release and incorporation into the cell.

A problem with this redox hypothesis is that the significantly negative redox potentials reported for the siderophores (Table 1) seemingly precludes reduction by a biological reducing agent such as NADH or NADP, which has a redox potential $\cong -320$ mV at neutral pH. (The tetradentate siderophores provide some advantage here as a result of their higher redox potentials. This suggests consideration of hexadentate siderophore ligand hydrolysis followed by redox and ligand exchange as another redox related iron release mechanism.) We have noted that the negative Fe(III/II) redox potential provides the basis for the high siderophore selectivity for Fe(III) among environmental metal ions (Equation 11), and removes the Fe-siderophore couple from the region which may catalyze the Haber-Weiss cycle to generate toxic reactive oxygen species (ROS) (Figure 7). However, by coupling competitive ligand exchange with an Fe(II) chelator and Fe(III)-siderophore reduction, the effective redox potential for a Fe(III/II) siderophore can be shifted into the range where reduction by NADH may readily occur. For example, although ferrioxamine B has a thermodynamic redox potential of -480 mV/NHE, the presence of a Fe(II) chelator with $\beta^{Fe(II)} \cong 10^{13}$ will shift the effective redox potential

above −300 mV, well into the region where reduction by NADH becomes thermodynamically feasible.

We propose that the redox process be considered as part of a *molecular switch*. In this model, when iron is in transit and needs to maintain a constant immediate chemical environment (inner coordination shell) for solubilization, transport and molecular recognition by the cell, it is in the +3 oxidation state. When the chemical environment must change (iron incorporation into the internal workings of the cell or movement to an alternate carrier) the iron oxidation state is changed to +2. This reduction may be facilitated by a coupled chelation reaction which scavenges the Fe(II) (Equations 19–20). Coupling Fe(III/II) redox to a ligand exchange reaction allows the overall process of iron release to function as a *synergistic switch*. Linking a ligand exchange process to a reductive electron transfer process can shift the '*effective*' redox potential positive – that is to make the Fe(III) thermodynamically easier to reduce. The *thermodynamic* redox potential for the Fe-siderophore complex is a measure of the *sensitivity of this switch*. The more negative the potential, the greater the difference between the siderophore affinity for Fe(III) and Fe(II) ($\beta^{Fe(III)}$ and $\beta^{Fe(II)}$; see Equation 11) and presumably the greater the change in iron lability on reduction (see Figure 7).

Acknowledgements

Research support for our work in this area from the National Science Foundation and the American Chemical Society Petroleum Research Foundation is gratefully acknowledged. We thank S. Dhungana and J.I. Wirgau, Duke University, for helpful discussions.

References

Albrecht-Gary A-M, Blanc S, Rochel N, Ocaktan AZ, Abdallah MA. 1994 Bacterial iron transport: Coordination properties of pyoverdin paA, a peptidic siderophore of pseudomonas aeruginosa. *Inorg Chem* **33**, 6391–6402.

Albrecht-Gary A-M, Crumbliss AL. 1998 Coordination chemistry of siderophores: Thermodynamics and kinetics of iron chelation and release. *Metal Ions Biol Syst* **35**, 239–327.

Albrecht-Gary A-M, Crumbliss AL. 1999 Siderophore mediated microbial iron bioavailability: A paradigm for specific metal ion transport. In: *Scientific Bridges for 2000 and Beyond.* Paris: Académie des Sciences, Editions TEC & DOC; pp. 73–89.

Anderegg G, L'Eplattenier F, Schwarzenbach G. 1963 Hydroxamate complexes. III. Iron(III) exchange between sideramines and complexones. A discussion of the formtion constants of the hydroxamate complexes. *Helv Chim Acta* **46**, 1409–1422.

Bickel H, Hall GE, Keller-Schierlein W, Vischer E, Wettstein A. 1960 Stoffwechselprodukte von Actinomyceten 27 Mitteilung. Uber die konstitution von ferrioxamin B. *Helv Chim Acta* **43**, 2129–2138.

Biruš M, Bradic Z, Krznaric G, Kujundžić N, Pribanic M, Wilikins PC, Wilkins RG. 1987 Kinetics of stepwize hydrolysis of ferrioxamine B and of formation of differrioxamine B in acid perchlorate solution. *Inorg Chem* **26**, 1000–1005.

Biruš M, Kujundžić N, Pribanić M 1993. Kinetics of complexation of iron(III) in aqueous solution. *Prog React Kinet* **18**, 171–271.

Boukhalfa H, Brickman TJ, Armstrong SK, Crumbliss AL. 2000 Kinetics and mechanism of iron(III) dissociation from the dihydroxamate siderophores alcaligin and rhodotorulic acid. *Inorg Chem* **39**, 5591–5602.

Boukhalfa H, Crumbliss AL. Unpublished results.

Boukhalfa H, Crumbliss AL. 2000 Multiple-path dissociation mechanism for mono- and dinuclear tris(hydroxamato)iron(III) complexes with dihydroxamic acid ligands in aqueous solution. *Inorg Chem* **39**, 4318–4331.

Boukhalfa H, Crumbliss AL. 2001 Kinetics and mechanism of a catalytic chloride ion effect on the dissociation of model siderophore hydroxamate-iron(III) complexes. *Inorg Chem* **40**, 4183–4190.

Bradbeer C. 1993 The proton motive force drives the outer membrane transport of cobalamin in *Escherichia coli*. *J Bacteriol* **175**, 3146–3150.

Braun V. 1998 Pumping iron through cell membranes. *Science* **282**: 2202–2203.

Braun V, Hantke K, Köster W. 1998 Bacterial iron transport: Mechanism, genetics and regulation. *Metal Ions Biol Syst* **35**, 67–145.

Buchanan SK, Smith BS, Venkatramani L, Xia D, Esser L, Palnitkar M, Chakraborty R., van der Helm D, Deisenhofer J. 1999 Crystal structure of the outer membrane active transporter FepA from *Escherichia coli*. *Nature Struct Biol* **6**, 56–63.

Caldwell CD, Crumbliss AL. 1998 Molecular recognition of ferrioxamine B by host-guest complex formation with lasalocid A in chloroform. *Inorg Chem* **37**, 1906–1912.

Carrano CJ, Cooper SR, Raymond KN. 1979 Coordination chemistry of microbial iron transport compounds. 11. Solution equilibrium and electrochemistry of ferric rhodotorulate complexes. *J Am Chem Soc* **101**, 599–604.

Caudle MT, Stevens RD, Crumbliss AL. 1994a Electrospray mass spectrometry study of 1:1 ferric dihydroxamates. *Inorg Chem* **33**, 843–844.

Caudle MT, Stevens RD, Crumbliss AL. 1994b A monomer-to-dimer shift in a series of 1:1 ferric dihydroxamates probed by electrospray mass spectrometry. *Inorg Chem* **33**, 6111–6115.

Clarke TE, Ku S-Y, Dougan DR, Vogel HJ, Tari LW. 2000 The structure of the ferric siderophore binding protein FhuD complexed with gallichrome. *Nature Struct Biol* **7**, 287–291.

Cooper SR, McArdle JV, Raymond KN. 1978 Siderophore electrochemistry: Relation to intracellular iron release mechanism. *Proc Natl Acad Sci USA* **75**, 3551–3554.

Dhungana S, Crumbliss AL. 2001 Microbial iron transport via a siderophore shuttle: A membrane ion transport paradigm. *ChemTracts-Inorg Chem* **14**, 258–265.

Dhungana S, White PS, Crumbliss AL. 2001 Crystal structure of ferrioxamine B: A comparative analysis and implications for molecular recognition. *J Biol Inorg Chem* **6**, 810–818.

Dhungana S, Heggemann S, Gebhardt P, Möllmann U, Crumbliss AL. 2002 Fe(III) coordination properties of a new saccharide-based exocyclic trihydroxamate analogue of ferrichrome. *Inorg. Chem.* submitted for publication.

Dodgen HW, Liu G, Hunt JP. 1981 Water exchange with ferric ion and oligomerized iron in acidic aqueous solutions. *Inorg Chem* **20**, 1002–1005.

Ducommun Y, Newman KE, Merbach AE. 1980 High-pressure O-17 NMR evidence for gradual mechanistic change over from I_a to I_d for water exchange on divalent octahedal metal ions from manganese(II) to nickel(II). *Inorg Chem* **19**, 3696–3703.

Ferguson AD, Hofmann E, Coulton JW, Diederichs K, Welte W. 1998 Siderophore-mediated iron transport: Crystal structure of FhuA with bound lipopolysaccharide. *Science* 282, 2215–2220.

Grant M, Jordan RB. 1981 Kinetics of solvent water exchange on iron(III). *Inorg Chem* **20**, 55–60.

Harris WR, Carrano CJ, Raymond KN. 1979 Coordination chemistry of microbial iron transport compounds. 16. Isolation, characterization, and formation constants of ferric aerobactin. *J Am Chem Soc* **101**, 2722–2727.

Helman R, Lawrence GD. 1989 The increase in ferrioxamine B reduction potential with increasing acidity of the medium. *J Electroanal Chem (Bioelectrochem Bioenergetics)* **22**, 187–196.

Hersman L, Lloyd T, Sposito G. 1995 Siderophore-promoted dissolutionof hematite. *Geochim Cosmochim Acta* **59**, 3327–3330.

Hersman L, Maurice P, Sposito G. 1996 Iron acquisition from hydrous Fe(III)-oxides by an aerobic Pseudomonas sp. *Chem Geol* **132**, 25–31.

Hersman LE. 2000 The role of siderophores in iron oxide dissolution. In Lovley DR ed *Environmental Microbe – Metal Interactions*, ASM, Washington DC; 145–157.

Hou Z, Raymond KN, O'Sullivan B, Esker TW, Nishio T. 1998 A Preorganized siderophore: Thermodynamic and structural characterization of alcaligin and bisucaberin, microbial macrocyclic dihydroxamate chelating agents. *Inorg Chem* **37**, 6630–6637.

Hou Z, Sunderland CJ, Nishio T, Raymond KN. 1996 Preorganization of ferric alcaligin, Fe_2L_3. The first structure of a ferric dihydroxamate siderophore. *J Am Chem Soc* **118**: 5148–5149.

Kadner RJ (1990) Vitamin B_{12} transport in *Escherichia coli*: Energy coupling between membranes. *Mol Microbiol* **4**, 2027–2033.

Konetschny-Rapp S, Jung G, Raymond KN, Meiwes J, Zaehner H. 1992 Solution thermodynamics of the ferric complexes of new deferrioxamine siderophores obtained by directed fermentation. *J Am Chem Soc* **114**, 2224–2230.

Larsen RA, Myers PS, Skare JT, Seachord CL, Darveau RP, Postle K. 1996 Identification of TonB homologs in the family enterobacteriaceae and evidence for conservation of TonB-dependent energy transduction complexes. *J Bacteriol* **178**, 1363–1373.

Lee CW, Ecker DJ, Raymond KN. 1985 Coordination chemistry of microbial iron transport compounds. 34. The pH-dependent reduction of ferric enterobactin probed by electrochemical methods and its implications for microbial iron transport. *J Am Chem Soc* **107**, 6920–6923.

Lincoln SN, Merbach AE. 1995 Substitution reactions of solvaled metal ions. *Adv Inorg Chem* **42**, 1–181.

Locher KP, Rees B, Koebnik R., Mitschler A., Moulinier L, Rosenbush JP, Moras D. 1998 Transmembrane signaling across the ligand-gated FhuA receptor: Crystal structures of free and ferrichrome-bound states reveal allosteric changes. *Cell* **95**, 771–778.

Loomis LD, Raymond KN. 1991 Solution equilibria of enterobactin and metal-enterobactin complexes. *Inorg Chem* **30**, 906–911.

Martell AE, Smith RM. 1974, 1975, 1976, 1977, 1982, 1989 Critical Stability Constants. Plenum, New York, Volumes 1–6.

Matzanke BF, Berner I, Bill E, Trautwein AX, Winkelmann G. 1991 Transport and utilization of ferrioxamine-E-bound iron in *Erwinia herbicola (Pantoea agglomerans)*. *BioMetals* **4**, 181–185.

Maurice PA, Vierkorn MA, Hersman LE, Fulghum JE, Ferryman A. 2001 Enhancement of kaolinite dissolution by an aerobic *Pseudomonas mendocina* bacterium. *Geomicrobiol J* **18**, 21–35.

Monzyk B, Crumbliss AL. 1982 Kinetics and mechanism of the stepwise dissociation of iron(III) from ferrioxamine B in aqueous acid. *J Am Chem Soc* **104**, 4921–4929.

Novicova NM, Novikov VT. 1981 Kinetics of complex formation by iron(III) with thyrone and 2,7-dichlorochromotropic acid. *Russ J Inorg Chem* **26**, 759–760.

Pecoraro VL, Harris WR, Wong GB, Carrano CJ, Raymond KN. 1983 Coordination chemistry of microbial iron transport compounds. 23. Fourier transform infrared spectroscopy of ferric catechoylamide analogues of enterobactin. *J Am Chem Soc* **105**, 4623–4633.

Postle K. 1993 TonB protein and energy transduction between membranes. *J Bioenerg Biomembr* **25**, 591–601.

Raymond KN, Carrano, CJ. 1979 Coordination chemistry and microbial iron transport. *Accts. Chem. Res.* **12**, 183–190.

Raymond KN, Mueller G, Matzanke BF. 1984 Complexation of iron by siderophores. A review of their solution and structural chemistry and biological function. *Top Curr Chem* **123**, 49–102.

Raymond KN, Telford JR. 1995 Siderophore-mediated iron transport in microbes. *NATO ASI Ser (Ser C)* **459**, 25–37.

Schalk IJ, Hennard C, Dugave C, Poole K, Abdallah MA, Pattus F. 2001 Iron-free pyoverdin binds to its outer membrane receport FpvA in *Pseudomonas aeroginosa*: a new mechanism for membrne iron transport. *Mol Microbiol* **39**, 351–360.

Schalk IJ, Kyslik P, Prome D, van Dorsselaer A, Poole K, Abdallah MA, Pattus F. 1999 Copurification of the FpvA ferric pyoverdin receptor of *Pseudomonas aeruginosa* with its iron-free ligand: Implications for siderophore-mediated iron transport. *Biochem* **38**, 9357–9365.

Schalk IJ, Abdallah MA, Pattus F. 2002 Recycling of Pyoverdin on the FpvA receptor after ferric pyoverdin uptake and dissociation in *Pseudomonas aeruginosa Biochem* **41**, 1663–1671.

Schwarzenbach G, Schwarzenbach K. 1963 Hydroxamate complexes. I. The stabilities of the iron(III) complexes of simple hydroxamic acids and desferriferrioxamine B. *Helv Chim Acta* **46**, 1390–1400.

Schwarzenbach G, Willi A. 1951 Metallindikatoren III. Die komplexbildung der brenzcatechin-3,5-disulfosaure (=Tiron) mit dem eisen(III)-ion. *Helv Chim Acta* **34**, 528–539.

Sigel A, Sigel H (eds). 1998 Iron Transport and Storage in Microorganisms, Plants and Animals. *Metal Ions in Biological Systems*, New York: Marcel Dekker, Inc.; Vol 35.

Spasojević I, Amstrong SK, Brickman TJ, Crumbliss AL. 1999 Electrochemical behavior of the Fe(III) complexes of the cyclic hydroxamate siderophores alcaligin and desferrioxamine E. *Inorg Chem* **38**, 449–454.

Spasojević I, Crumbliss AL. 1998 Bulk liquid membrane transport of ferrioxamine B by neutral and ionizable carriers. *J Chem Soc Dalton*, 4021–4027.

Spasojević I, Crumbliss AL. 1999 pH induced active ('uphill') liquid membrane transport of ferrioxamine B by the ionizable ionophore lasalocid. *Inorg Chem* **38**, 3248–3250.

Spasojević I, Crumbliss AL. 2002 Kinetics and mechanism of ferrioxamine E complex formation and dissociation in aqueous acid. *Inorg Chem*, in preparation.

Spasojević I, Boukhalfa H, Stevens RD, Crumbliss AL. 2001 Aqueous solution speciation of Fe(III) complexes with dihydroxamate siderophores alcaligin and rhodotorulic acid and synthetic analogues using electrospray ionization mass spectrometry. *Inorg Chem* **40**, 49–58.

Stintzi A, Barnes C, Xu J, Raymond KN. 2000 Microbial iron transport via a siderophore shuttle: A membrane ion transport paradigm. *Proc Natl Acad Sci USA* **97**, 10691–10696.

Stojiljkovic I, Sirinivasin N. 1997 Neisseria meningitidis TonB, ExbB and ExbD genes: TonB-dependent utilization of protein-bound iron in neisseriae. *J Bacteriol* **179**, 805–812.

Swaddle RW, Merbach AE. 1981 High-pressure oxygen-17 fourier transform NMR spectroscopy. Mechanism of water exchange on iron(III) in acidic aqueous solution. *Inorg Chem* **20**, 4212–4216.

Telford JR, Raymond KN. 1996 Molecular recognition: Receptors for cationic guests. In: Atwood JL, Davies JED, MacNicol DD, Voegtle F eds. *Comprehensive Supramolecular Chemistry*. Oxford: Elsevier Science; 245–266.

Trzaska SM, Kim M, Bartsch RA, Crumbliss AL. 2001 Optimization of the lariat ether carboxylic acid host structure for a ferrioxamine B guest: Demonstration of a second coordination shell chelate effect. *Inorg Chem* **40**, 5823–5828.

Trzaska SM, Toone EJ, Crumbliss AL. 2000 Microcalorimetric determination of thermodynamic parameters for ionophore-siderophore host-guest complex formation. *Inorg Chem* **39**, 1071–1075.

van der Helm D. 1998 The physical chemistry of bacterial outer-membrane siderophore receptor proteins. *Metal Ions Biol Syst* **35**, 355–401.

Wawrousek EF, McArdle JV. 1982 Spectroelectrochemistry of ferrioxamine B, ferriochrome, and ferrichrome A. *J Inorg Biochem* **17**, 169–183.

Winkelmann G (ed). 1991 *Handbook of Microbial Iron Chelates*. Boca Raton, FL: CRC Press.

Winkelmann G, Carrano CJ. (eds) 1997 *Transition Metals in Microbial Metabolism*. The Netherlands: Harwood Acad. Publ.

Wirgau JI, Spasojević I, Boukhalfa H, Batinic-Haberle I, Crumbliss AL. 2002 Thermodynamics, kinetics and mechanism of the stepwise dissociation and formation of tris(L-lysinehydroxamato)iron(III) in aqueous acid. *Inorg Chem* **41**, 1464–1473.

Wong GB, Kappel MJ, Raymond KN, Matzanke B, Winkelmann G. 1983 Coordination chemistry of microbial iron transport compounds. 24. Characterization of coprogen and ferricrocin, two ferric hydroxamate siderophores. *J Am Chem Soc* **105**, 810–815.